Energy Harvesting and Pavement Sensing for Enhanced Life of Pavement Structures

Final Report
November 2020

Principal Investigator: K. Wayne Lee

Department of Civil and Environmental Engineering
University of Rhode Island

K. Wayne Lee
Michael L. Greenfield
Austin DeCotis
David Schumacher
Kevin Lapierre

Sponsored By
Transportation Infrastructure Durability Center

University of Rhode Island
College of Engineering
2 East Alumni Avenue
Kingston, RI 02881
(401)874-2695
https://web.uri.edu/ritrc/

About the Transportation Infrastructure Durability Center

The Transportation Infrastructure Durability Center (TIDC) is the 2018 US DOT Region 1 (New England) University Transportation Center (UTC) located at the University of Maine Advanced Structures and Composites Center. TIDC's research focuses on efforts to improve the durability and extend the life of transportation infrastructure in New England and beyond through an integrated collaboration of universities, state DOTs, and industry. The TIDC is comprised of six New England universities, the University of Maine (lead), the University of Connecticut, the University of Massachusetts Lowell, the University of Rhode Island, the University of Vermont, and Western New England University.

U.S. Department of Transportation (US DOT) Disclaimer

Acknowledgements

Funding for this research is provided by the Transportation Infrastructure Durability Center at the University of Maine under grant 69A3551847101 from the U.S. Department of Transportation's University Transportation Centers Program. Authors would like to acknowledge the cooperation and support by University of Rhode Island (URI) including Dr. Peter Snyder, Mr. Kevin Broccolo, and Ms. Kelly Stanzion, and Rhode Island Department of Transportation including Mr. Steven Cascione Technical Champion.

Technical Report Documentation Page

1. Report No.	**2. Government Accession No.**	**3. Recipient Catalog No.**
4 Title and Subtitle Energy Harvesting and Pavement Sensing for Enhanced Life of Pavement Structures		**5 Report Date** November 8, 2020 **6 Performing Organization Code**
7. Author(s) K. Wayne Lee https://orcid.org/0000-0002-5204-9493 Michael L. Greenfield https://orcid.org/0000-0002-4704-1489		**8 Performing Organization Report No.** RITRC 20-1
9 Performing Organization Name and Address Rhode Island Transportation Research Center (RITRC) University of Rhode Island (URI) 2 East Alumni Avenue, Kingston, RI 02881		**10 Work Unit No. (TRAIS)** **11 Contract or Grant No.**
12 Sponsoring Agency Name and Address USDOT Region 1 University Transportation Center (UTC) – Transportation Infrastructure Durability Center (TIDC)		**13 Type of Report and Period Covered** **14 Sponsoring Agency Code**
15 Supplementary Notes		

16 Abstract

A solar energy harvesting system was examined to heat water using a proto-type asphalt pavement in the lab, but it was not efficient. Thus, a second approach was continued to create an efficient asphalt pavement solar collector using thermoelectric generators (TEGs). Thorough testing was needed to evaluate the implementation of the energy harvesting device into the roadway. The temperature difference between opposing TEG surfaces will generate the required voltage to operate the roadway sensors. Now that the solar harvester has been installed into the shoulder of a roadway, the ability of heat transfer to generate electrical energy needs to be tested in this real-world application. To bring heat to the TEGs from the asphalt surface layer, the harvester included an insulated copper plate that reached 25mm (1 in.) below the top layer. This allows temperature difference readings as well as maximum power output voltage. This copper plate will be heated from the sun heating the asphalt surface layer and transfer the energy into the harvester system. Calculations show that this heat transfer is reasonable if heat flow along the plate into deeper asphalt layers can be neglected.

17 Key Words Pavement sensing, Enhanced life of pavement, Solar energy harvesting, Thermoelectric generator, Heat transfer		**18 Distribution Statement** No restrictions. This document is available to the public through	
19 Security Classification (of this report) Unclassified	**20 Security Classification (of this page)** Unclassified	**21 No. of pages**	**22 Price**

Form DOT F 1700.7 (8-72)

Contents

List of Figures 4
List of Tables 4
Abstract 5
Chapter 1: Introduction and Background 6
1.1 Project Motivation 6
1.2 Research, Objectives, and Tasks 6
1.3 Report Overview 7
Chapter 2: Energy Harvesting and Advanced Technologies for Enhanced Life 8
2.1 Introduction 8
2.2 Energy Harvesting with Embedded Heat-Conductive Piping Methods 9
2.3 Results and Analysis 11
2.4 Discussion 14
2.5 Summary 15
Chapter 3: Energy Harvesting and Advanced Technologies for Road Assessment Tools 16
3.1 Methodology 16
3.2 Apparatus to Harvest Solar Energy 16
3.3 Apparatus to Use Solar Energy – Strain Sensing as an Example 19
3.4 Procedure to Build Solar Harvester 21
3.5 Cost Analysis 21
3.6 Procedure to Install Solar Harvester and Sensor in the Field 22
3.7 Verification Before Field Installation 23
3.8 Installation 24
3.9 Strain Measurement 26
3.10 Summary and Future Works 27
Chapter 4: Thermodynamic Analysis of Solar Energy Harvesting Processes 29
4.1 Finite Element Modeling of Heat Flow from Asphalt into a Cooling Water Pipe 29
4.2 Theoretical Efficiency of Extracting Heat from Asphalt as Work 30
4.3 Modeling of Energy Added to Cooling Water by a Pump 30
4.4 Example of Heat Flow Condition during Thermoelectric Energy Harvesting 32
4.5 Example of Heat Flow Dynamics during Energy Harvesting 33
4.6 Conclusions from Modeling 35
Chapter 5: Conclusions and Recommendations 36
References 38

List of Figures

Figure 2.1 Apparatus for embedded heat-conductive piping
Figure 2.2 Average asphalt temperatures at different depths
Figure 2.3 Water testing data and ambient temperature
Figure 2.4 Legends for Figure 2.5
Figure 2.5 Data for pavement structure, water, and ambient temperature
Figure 2.6 100 mm (4 in.) depth vs ambient temperature vs water temperature
Figure 3.1 Solar energy harvesting system
Figure 3.2 Dynatest Wheatstone bridge connection sensor
Figure 3.3 Cross section of solar harvester, embedded in shoulder of road 25 mm (1 in.) below asphalt surface
Figure 3.4 Connection between TEGs, Booster converter, Arduino Uno, Amplifier, and load cell Sensor
Figure 3.5 Temperature of the hot side of TEG with its corresponding voltage, ambient air temperature 23°C (74°F)
Figure 3.6 Plans for the location, layout, and geometry of the installed energy harvester and strain sensor on Plains Road in Kingston, RI
Figure 3.7 Markings for the saw cuts for strain sensor (in the road) and energy harvester (in the shoulder) on Plains Road in Kingston, RI
Figure 3.8 Designing a hole for the irrigation box in the shoulder of Plains Road.
Figure 4.1 Calculated temperature profile for asphalt around a cooling pipe
Figure 4.2 Model results for temperature within the vertical copper plate, assuming perfect insulation along the sides and an instantaneous rise to 140°F at the top

List of Tables

Table 3.1 Characteristics of Dynatest PAST sensor
Table 3.2 Costs of solar harvest and sensors
Table 4.1 Heat capacity parameters for water
Table 4.2 Calculation results for pump energy input

Abstract

A solar energy harvesting system was examined to heat water using a proto-type asphalt pavement in the lab, but it was not efficient. Thus, a second approach was continued to create an efficient asphalt pavement solar collector using thermoelectric generators (TEGs). Thorough testing was needed to evaluate the implementation of the energy harvesting device into the roadway. The temperature difference between opposing TEG surfaces will generate the required voltage to operate the roadway sensors. Now that the solar harvester has been installed into the shoulder of a roadway, the ability of heat transfer to generate electrical energy needs to be tested in this real-world application. To bring heat to the TEGs from the asphalt surface layer, the harvester included an insulated copper plate that reached 25mm (1 in.) below the top layer. This allows temperature difference readings as well as maximum power output voltage. This copper plate will be heated from the sun heating the asphalt surface layer and transfer the energy into the harvester system. Calculations show that this heat transfer is reasonable if heat flow along the plate into deeper asphalt layers can be neglected.

Chapter 1: Introduction and Background

1.1 Project Motivation

The properties of asphalt pavement allow the accumulation and dissipation of solar energy on a daily cycle. Heat is absorbed in pavements, causing many detrimental effects such as the degradation of pavement, heat island effect, and increased costs for cooling nearby structures (Lee et al. 2010; Lee and Kohm 2014). Harvesting solar energy from pavement has the potential to provide many substantial benefits such as extending the service life of pavements, improving the air quality, lowering impacts to the climate, and producing energy (Lee and Correia 2010). The Rhode Island Transportation Research Center (RITRC) team at the University of Rhode Island (URI) investigated important aspects of energy harvesting via an embedded solar harvester system, which was created to reduce pavement distresses and to enhance evaluating pavement performance (Lee and Correia 2011; Lee et al. 2012a).

Typically, sun shining on pavement provides it with thermal energy throughout the day. Past studies have confirmed that pavement temperature rises and falls each day, and the magnitude of the daily fluctuations varies with albedo (fraction of reflected sunlight), light absorption by the pavement, and emission, all of which can vary with latitude, with season of the year, and with the pavement itself (Han et al. 2011). Pavement temperature falls at night as it radiates heat back into the atmosphere and as heat is conducted into underlying layers and subgrade soils.

Harvesting energy from pavement refers to injecting engineered processes into this daily thermal cycle. The goal is to capture part of the daily energy flow and to channel it to other uses. The benefits cited above for energy harvesting arise from the lower temperatures that can result from extracting energy from pavement more quickly than can be obtained in a typical daily cycle.

1.2 Research, Objectives, and Tasks

In year 1 of this project, direct heat transfer was pursued as a harvesting strategy. Water was circulated via pipes through an asphalt core in a laboratory environment. The hypothesis was that heat would flow into the pipe and water, cooling the pavement. A challenge was how that warm water can be used. (The maximum water temperature is the highest pavement temperature.) There also was not an efficient way to cool the water so it could be recirculated and always start out being cold. Instead, the closed water system increased in temperature over time, and ultimately it added heat to some of the lower pavement layers, rather than removing heat. An external pump moved the water through the pipes, so ultimately this system consumed useful energy while extracting low grade thermal energy that needed to be transferred somewhere else. It did not harvest energy in a sustainable, effective manner, unless warm water can used externally.

During year 2, research and development efforts focused on building an apparatus that can harvest thermal energy from a pavement by a *thermoelectric* approach rather than relying on harvesting thermal energy directly. Opposing semiconductors in a "thermoelectric generator" create electrical voltage when they are brought to different temperatures (Lee et al. 2012b). A ceramic barrier provides electrical

insulation between the opposing surfaces and also cuts down on direct heat transfer. Instead, energy flows from higher to lower electrical potential through a wire, transferring the energy electrically rather than thermally. This creates a possibility of harvesting energy by powering an external circuit with this voltage. The electrical power becomes available for use within the pavement itself.

1.3 Report Overview

Chapter 1 describes background and motivation for the research. Chapter 2 describes the research that employed direct heat transfer into a water pipe from asphalt mix. Chapter 3 describes energy harvesting by using the thermoelectric approach. Chapter 4 describes modeling work that supported the experiments described in chapters 2 and 3. Chapter 5 provides a summary and recommendations regarding how these Energy Harvesting strategies address Advanced Technologies for Enhanced Life.

Chapter 2: Energy Harvesting and Advanced Technologies for Enhanced Life

The RITRC at the URI has been working to create a solar energy harvesting system for asphalt pavement. The first objective was to cool pavement structures effectively on hot days, which will thus increase the service life of the pavement. This will decrease the amount of rehabilitation, which will save time, money and energy. The second intention of the present study was harvesting as much solar energy as possible to create a more sustainable pavement. This energy could be used for a structural health monitoring system. If larger amounts of harvested energy become available, then a wide variety of uses include powering streetlights, ice melting, and traffic signals. The solar energy harvesting methods included extracting heat through embedded conductive piping and generating power via a temperature differential.

2.1 Introduction

As the population continues to expand, natural resources become less available and the growing need for renewable energy intensifies. Renewable energies are clean and inexhaustible. Fossil fuels are currently the largest energy source utilized but the impacts caused by them are real and devastating. The greenhouse gases created by the burning of fossil fuels continues to escalate the impacts of global warming. If the current trends of warming continue there will be catastrophic effects on the planet (Akbari 2005). Renewable energy sources which are very diverse and don't produce greenhouse gases are needed for the future (Lee and Kohm 2014). Of this diverse group of renewable energy, one of the most important is solar energy (Lee et al. 2010). Every day the sun shines, heating up the earth, and the potential for this solar energy harvesting is unlimited. It is a clean and safe energy source that can replace fossil fuels if enough energy is captured.

Solar energy has been collected through solar panels, which can be placed in almost any location that receives sunshine. The more surface area a solar collector has, the more energy it collects. Many homeowners are starting to install solar panels on their roofs to power their own homes in the US and around the world. Panels are also installed in fields, on industrial buildings and even floating on water. The only negative to panels is that they take up a lot of space.

To further increase the harvesting of solar energy, more surface area for solar harvesting needs to be utilized. In the US there are millions of miles of roadways and parking lots, and an opportunity has arisen for multi-functionalization besides automobile traveling. The sun's ultraviolet rays penetrate these roadways every day. These roadways provide a large amount of surface area, and they would be ideal for solar harvesting if the unit can withstand the reoccurring loads of daily truck traffic. If all the surface area of the roadways in the U.S. were utilized effectively for solar harvesting, fossil fuel consumption could plummet, which would lead to a cleaner and healthier society (Lee and Correia 2011).

On hot and sunny days, the roadways in the U.S reach up to 60ºC (140ºF). This high temperature is favorable for solar energy harvesting, yet it is extremely detrimental to the roadway structure. The increased heat in pavement leads to the phenomenon called heat island effect. The pavement absorbs the sun's heat and traps the heat so urban and city areas with lots of paved roadways tend to stay warmer. This

in turn leads to higher air conditioning costs in cities during the summer and a possible contribution to climate change. The high temperatures in the asphalt pavement also lead to rutting. This greatly decreases the life of pavement, which leads to expensive and energy intensive repairs.

The RITRC at the URI has been working to create a solar energy harvesting system for asphalt pavement. The idea behind this is to cool the pavement effectively on hot days, which will therefore increase the service life of the pavement. This will lead to fewer repairs, saving money and energy. A second and more essential idea of this study will be harvesting as much solar energy as possible to create a more sustainable pavement. This energy could be used for a wide variety of uses including powering streetlights, ice melting, traffic signals and structural health monitoring systems, if enough power could be obtained.

2.2 Energy Harvesting with Embedded Heat-Conductive Piping Methods

RITRC previously conducted a study on harvesting solar energy in asphalt pavement by embedding conductive piping in asphalt pavements (Lee and Correia 2010; Lee et al. 2012b). The objectives were to investigate novel methods to harvest solar energy from asphalt pavement, to generate different approaches to capture solar energy, to formulate conceptual design of systems to generate electricity and to determine the feasibility of the studied novel methods. A prototype system was developed that utilized a 25 cm (10 in.) diameter by 60 cm (24 in.) tall clear schedule 40 PVC cylinder to simulate the pavement structure used in most roadways in Rhode Island (RI). This cylinder had 12.5 cm (5 in.) of subgrade soils, a 30 cm (12 in.) granular sub-base, 7.5 cm (3 in.) asphalt base, 5 cm (2 in.) asphalt binder course and a 5 cm (2 in.) asphalt surface course from the bottom. This was the minimum thickness within RI Department of Transportation (DOT) standard specifications at the time. To measure the temperature of the pavement structure accurately, 10 thermocouples were embedded in the pavement at varying depths. Cross-linked polyethylene (PEX) tubing was embedded 10 cm (4 in.) below the asphalt surface. This piping was chosen due to characteristics such as cost effectiveness, flexibility, melt resistance, and freeze cracking resistance. Since this experiment was performed in a laboratory, the field conditions of the pavement had to be simulated. An incandescent light bulb as a heat and light source was situated such that pavement surface temperature peaked at 140ºF. A pump was used to circulate water through the PEX pipe.

In the present work, the RITRC team thoroughly analyzed that prior pilot study to determine sources of error. One omission that stood out was the energy added into the water through operating the pump. It is known that energy is contributed directly by adding kinetic energy to move water and indirectly through losses and inefficiencies, which convert mechanical energy added to the system into heat. The heat generated by the pump was not accounted for in the last study. The exact make and model of the pump used in the last experiment is unknown. A similar pump was used for this study, and a preliminary analysis quantified the large amount of heat that the pump adds into the water.

Before testing data on pavement cooling were recorded, a baseline was established. A 60W light bulb was used as a heat source. Control testing started with the light bulb at 30 cm (12 in.) above the pavement apparatus. Multiple iterations of this control testing were run until the desired pavement surface temperature of approximately 60ºC (140ºF) was achieved by placing the light bulb 75mm (3 in.) above the pavement surface. The light bulb was run for a 12 hour on / 12 hour off cycle for two days in a row.

These control data were used to compare with testing data under water flow conditions. To analyze the water and to account for the energy contributed by the pump, further control testing was performed. The pump was run for 12 hours and switched off for 12 hours for three consecutive days.

Figure 2.1 shows the basic set up. There are two apparatuses here. The one with the blue piping was used in the 2012 study. The apparatus with the red piping was created for the present study. For control testing, water was pumped through the old apparatus to measure the rise in temperature due to the pump. At the same time, the new cylinder was heated with the lamp. Temperature data for the water were collected along with data for various depths in the pavement sample. Three days of data were collected for the water control data. Two days of data were collected for the pavement control data. The quantity of water used in the holding tank was 5,000mL and was pumped at a rate of approximately 5 gallons/minutes.

Once good control data were collected, the cooling experiment was started 12 hours later. The second apparatus with the blue piping was removed and the pump was now connected to the new apparatus with red piping. The lightbulb was once again set to run for 12 hours and then shut off for 12 hours. The pump was set to turn on 30 minutes after the light bulb turned on to allow the apparatus to heat up. The pump would then run for 12 hours and then shut off for 12 hours. This cycle was completed for 7 consecutive days. Temperatures as a function of depth and time constitute the results.

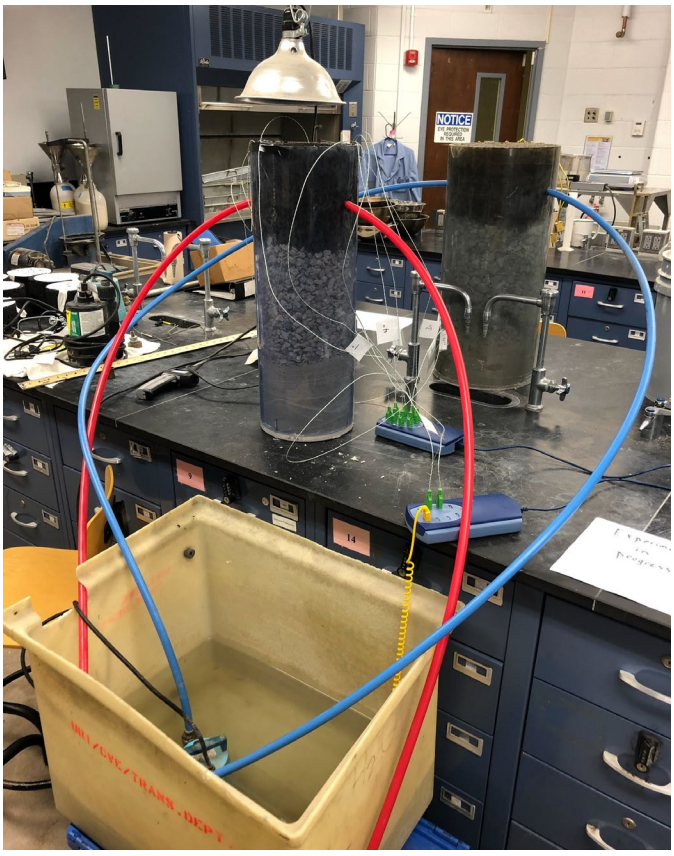

Figure 2.1. Apparatus for embedded heat-conductive piping.

2.3 Results and Analysis

Average Asphalt Temperature Analysis

Figure 2.2 shows the average monitored temperature at different depths in the laboratory pavement structure. These data were taken during the common day while a pumping system is engaged, and they include average temperature of water that enters the pump. The asphalt samples that had water run through the embedded pipes reached lower peak temperatures at every layer in the asphalt sample other than in the subgrade soils, and they cooled down faster compared to the testing that was performed without water. The temperature of the water increased from 19°C (67°F) to 33°C (91°F) over the period of 8 hours while the system was run (Figure 2.1). This indicates that energy can be harvested from the pavement using embedded piping. However, our recent testing suggests that nearly 50% of this temperature rise was input to the water as heat from the pump. The pump as a heat source explains how the water temperature could rise above the temperature of the surrounding pavement. This was a small-scale experiment, with only 20cm (8 in.) of piping embedded in the pavement. Heat was also lost through the pipe as it traveled from the asphalt sample to the holding tank. Earlier results (Lee and Correia 2010) suggest that if this experiment was done on a larger scale with miles of roadway, then there is potential to harvest a massive amount of heat. Larger scales would also increase pump energy input requirements, however.

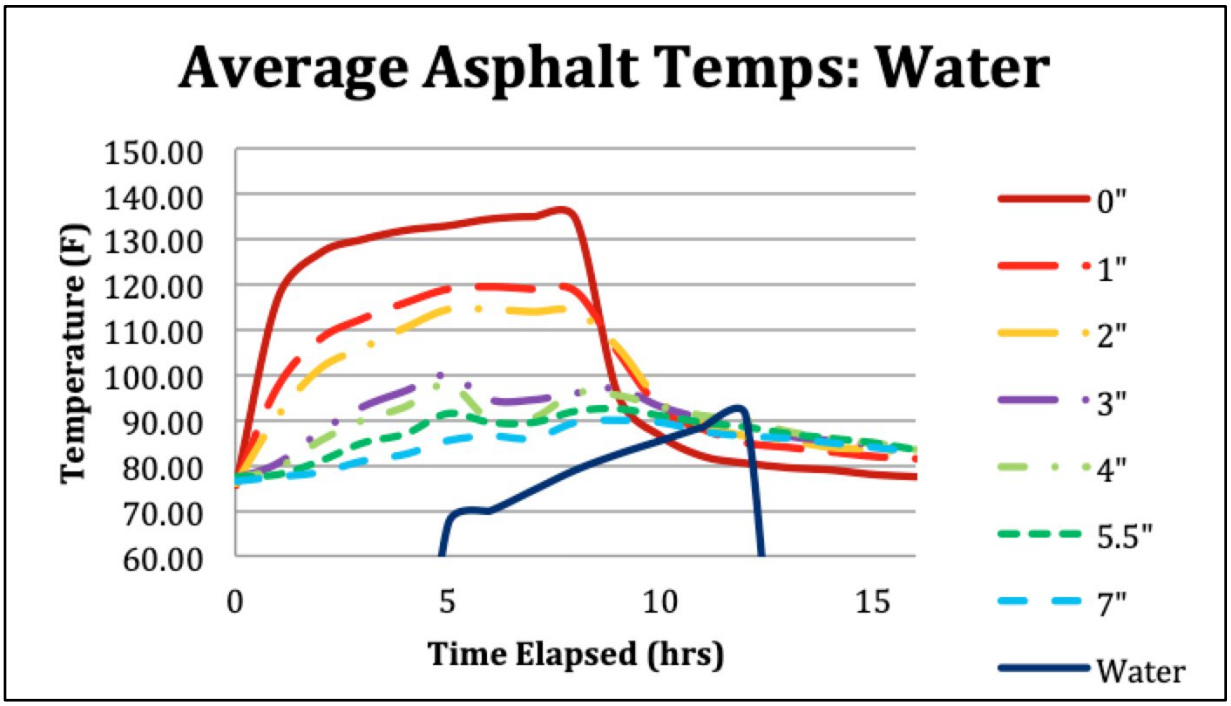

Figure 2.2. Average Asphalt Temperatures at different depths

Figure **2.3** displays the data recorded by the thermocouple placed inside the water holding tank and the ambient temperature. Control testing started on Wednesday May 22nd, 2019 and ran for three cycles. The pump was on during the first half of each cycle and the lamp was off throughout these cycles. The temperature rise during pumping indicates that the pump input a very large amount of heat into the water.

The water reservoir temperature increased approximately 15ºC (27ºF) on average just from the heat of the pump. Starting on the morning of Saturday the 25th, the pump was connected to the apparatus that was being heated by the light bulb. The goal of this was to see if the water reservoir would raise to a higher temperature by absorbing the heat from the pavement. The experiment was run for the next 7 days. The data over these cycles in Figure **2.3** show that no substantial heat gain in the water arose due to the added heat of the pavement. Even on days with higher ambient temperatures, the temperature of the water still reached approximately the same peak temperature of 35ºC (95ºF). This suggests that nearly all the heat input into the water was due to heat caused by the pump.

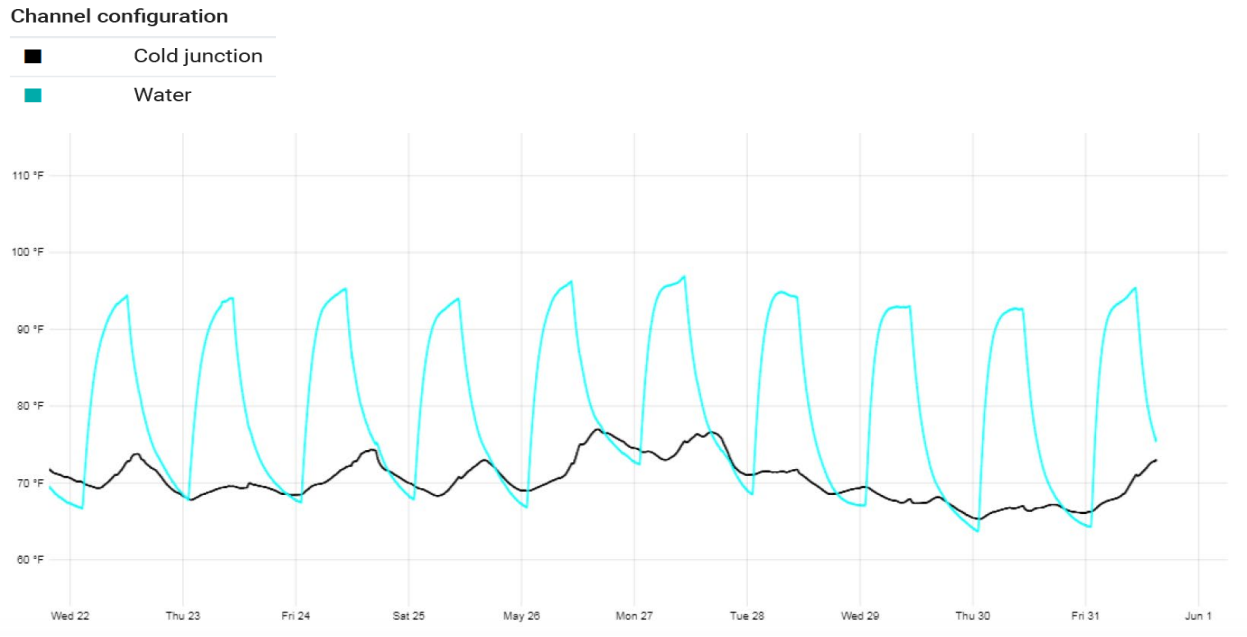

Figure 2.3: Water testing data and ambient temperature

The temperature of the pavement structure was next analyzed. Figure 2.4 displays the legend for Figure **2.5**, which shows the results of the data from the experiment. The control data for the pavement structure were collected for two days starting on Thursday, March 28, 2019. For these data, the light was turned on for 12 hours to simulate the sun. The light was then turned off for 12 hours to simulate nighttime. This was done for two cycles to get control data to see exactly how hot each layer of pavement got without any water being pumped through the PEX piping. The data for the water control testing were also included in Figure *2.5* to compare it to the temperatures of the pavement sample. The first day of water control testing was omitted as there was one less day of control testing for the pavement sample. It is noted that in Figure 2.5 the color of the line for the water data has changed to blue color as opposed to cyan color in Figure 2.3.

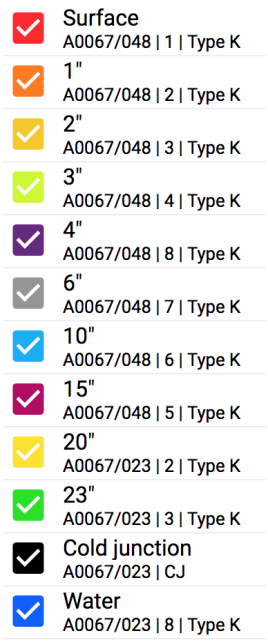

Figure 2.4: Legend for Figure 2.5

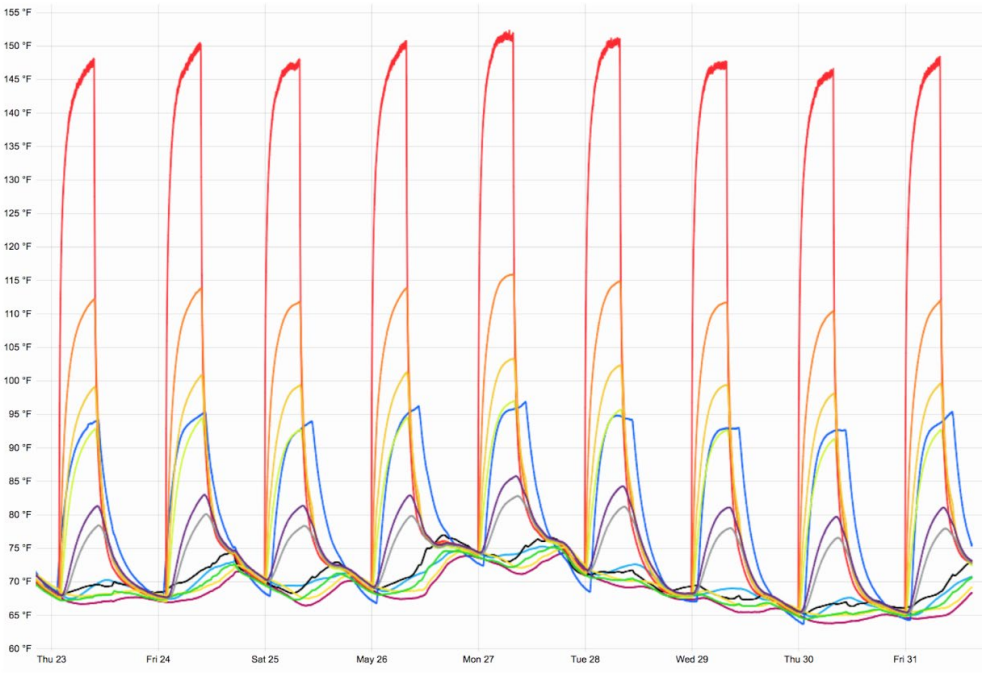

Figure 2.5: Data for Pavement Structure, Water and Ambient Temperature

Directly after the control testing was completed on the morning of Saturday, May 25, the pump was hooked up to the heated pavement apparatus. The light bulb was illuminated for 12 hours and turned off

for 12 hours. The pump was set to turn on 30 minutes after the light bulb was turned on. The pump also followed the 12 hours on and 12 hours off schedule. This cycle continued for 7 days.

Starting with the data for the surface temperature, it is shown in Figure 2.5 that the surface temperatures for the pavement were very similar for each day. The surface temperatures did not decrease compared to the control testing. This concludes that the water pumped through the pipes did not affect the surface temperature. This same trend is observed in all the remaining pavement layers also. These results were not expected; however, it is clear from the data that the pump was inputting most of the heat into the water and the water was not cooling the pavement structure.

2.4 Discussion

After observing unexpected results, the RITRC team looked back on what could explain this. After thorough examination, the large pump being utilized was rapidly causing the water to heat up so much that the temperature of the water quickly became hotter than the pavement directly surrounding where the pipe was placed in the pavement structure.

The pipe was placed at 100mm (4 in) below the pavement surface. A thermocouple was also placed at 100mm below the pavement structure and 12mm (0.5 in.) to the side of the pipe. During control testing (the testing without water being pumped through the pavement structure), the pavement layer at 100mm (4 in.) was only reaching peak temperatures of approximately 80ºF. However, during the control testing for the water, the pump was heating up the water to temperatures above 94ºF. With the temperature of the water already reaching much higher temperatures than the surrounding pavement, there is no possible way to cool down the pavement and to increase the temperature of the water. These data for water and for the pavement layer at 100mm (4 in.) are displayed in Figure 2.6 to emphasize the higher temperature of the water.

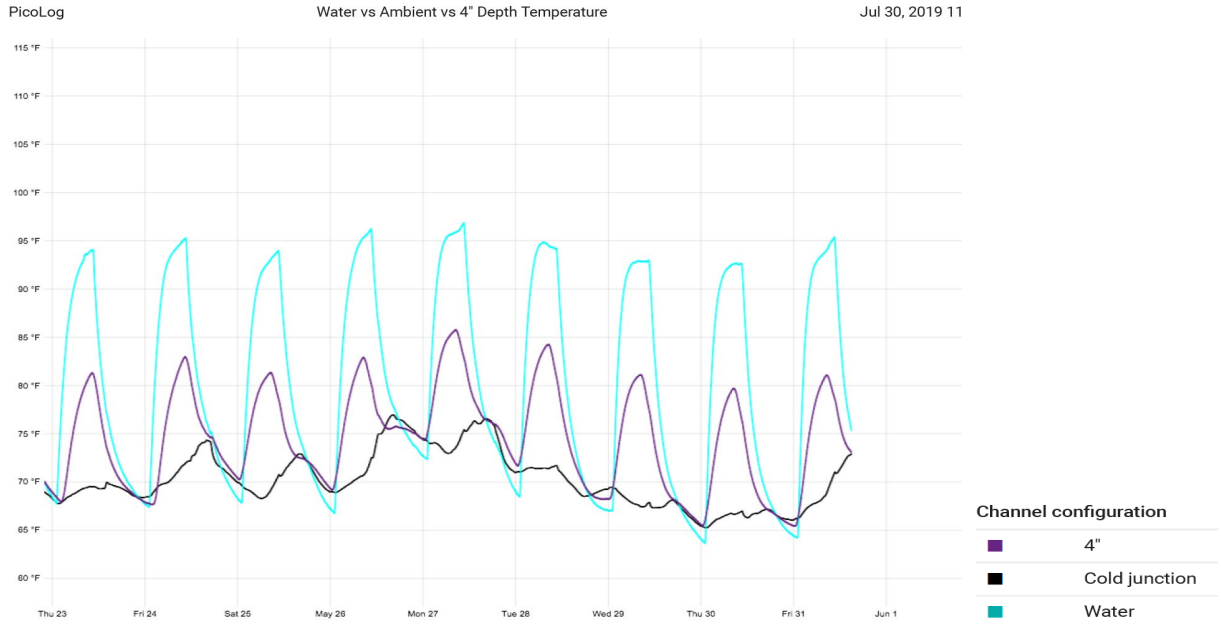

Figure 2.6: 100mm (4 in.) Depth vs Ambient Temperature vs Water Temperature

The RITRC team did not have optimum results with this experiment so far. There is still a possibility this method could work with future refinement. First and foremost, a smaller pump that puts out less heat would need to be used to determine if the heat of the pavement structure can increase the temperature of water. The size and heat output of this pump was a major source of error in this experiment. It is likely that a much smaller pump will be able to sufficiently pump water through this small-scale lab experiment. Due to time constraints, the RITRC team has not yet completed further testing with a new pump.

Another consideration that could make this experiment more efficient would be moving the height of the pipe in the pavement structure closer to the surface. This would increase the temperature of the pavement surrounding the pipe, which makes it more likely to increase the temperature of the water. However, in doing this it creates the potential for the embedded pipes to be damaged by traffic in a real-world situation. Moving the pipes any closer to the surface would likely require load testing to determine the structural adequacy of the setup.

The URI research team will continue to validate this system utilizing the embedded conductive piping. Research will also be continued to create an efficient asphalt pavement solar collector using thermoelectric generators. RITRC is currently performing similar experiments with hopes to optimize this method for widespread use, and these will be discussed in Chapter 3.

2.5 Summary

With more industries concentrating on greener technologies, different methods for energy harvesting can help utilize an untapped source of energy that is ignored every day. RITRC researchers of URI have been exploring solar energy harvesting from asphalt pavement as we believe it has a strong potential to be utilized among all roadways and contribute to a more sustainable world. With the current need to switch to more sustainable energy, it is best to look at all possible alternatives. Although these ideas are still new yet with research and development, they can hopefully be optimized for widespread future use.

Chapter 3: Energy Harvesting and Advanced Technologies for Road Assessment Tools

The URI research team is performing experiments utilizing the Seebeck Effect (Lee et al. 2012a; Yang et al 2005). The Seebeck principle comprises two dissimilar electrical conductors or semiconductors that have a difference in temperature, which produces a voltage difference between the two substances (Feng and Ellis 2003; Pinter et al. 2007). Recently, an experiment using the Seebeck principle was performed to develop a self-powered battery-less structural health monitoring (SHM) system for transportation infrastructure (Karsilaya et al. 2018). The system would be capable of processing analog voltage input from a variety of sensors, such as strain gauges, traffic counters and piezoelectric weighing strips (McCathy et al. 2000). An energy harvester driven by thermoelectric generators (TEGs) powered their system. TEGs function on the Seebeck/Peltier principle, allowing thermal differences between the upper and lower layers of asphalt concrete to be translated into electrical energy (Purohit et al. 2013). The surface heat of the pavement would be transferred from the surface to the lower layers through insulated copper plates, and the lower part of the harvester was kept cool through a heat sink (Racicot et al. 1997). Thermoelectric generators can power SHM systems when enough of a temperature differential exists to power the TEGs. This SHM system developed by the Texas A&M University (TAMU) team appeared to be successful. The system accepts analog voltage input from a variety of sensors, is readily programmable, functions without a storage battery, and can continuous retrieve wireless data. The URI research team has been conducting similar studies independently. Literature review utilizing the Seebeck/Peltier Effect (thermoelectric effect) was further researched and reviewed. An effort was made to harvest solar energy for developing a road performance assessment tool, as described below.

3.1 Methodology

The setup developed in year 2 study has two broad functions. The first setup harvests some of the thermal energy that is available by converting it into electric voltage. This provides a capability to do useful work in real time. The second setup uses the electrical power provided by the energy harvesting system in order to power a strain sensor. The sensor monitors pavement deformation or strains of passing traffic. This second setup involves conversion of the generated voltage into a steady flow that can operate the sensor and its electronics.

3.2 Apparatus to Harvest Solar Energy

Thermoelectric Generators

Thermoelectric generators (TEGs) power the system by translating a thermal difference in temperature between their upper and lower layers into electrical energy. They convert the environmental energy that exists in the form of a thermal gradient into electrical energy. Normally heat would flow down a temperature gradient in the form of thermal conduction. Instead, the TEG replaces that energy flow with a form of electrical energy that flows from a higher voltage to a lower voltage. This voltage that drives that electrical current can be directed through a circuit, which provides for extracting useful electrical work from the pavement.

The layers within a TEG consist of two different semi-conductor materials (p-type and n -type elements) between two ceramic substrates to generate voltage. As one side of the TEG becomes hot due to heat transfer from the upper pavement layer, the other same remains a colder temperature, allowing a voltage to be produced. A cartoon depicts the overall structure (Fig. 3.1a) and a photograph depicts the system during benchtop testing (Fig. 3.1b).

A TXL-287-03 TEG from TXL Group Inc was used in this study. It employs a bismuth telluride thermoelectric material. Further information is available at https://txlgroup.com/te-generators/ . Two TEGs in parallel were used in order to increase the available current.

Copper plate Apparatus

A first step is to deliver heat from the hot pavement surface to the TEGs that extract the useful energy. Normally this heat flows from surface to interior directly through the pavement. This creates a temperature gradient within the pavement that is incapable of allowing energy to be extracted. To circumvent this typical equilibrium, an easier path was created for channeling heat flow to the embedded TEGs. This took the form of a long, thin plate. The main experimental setup consists of an "L" shape design 470mm (18.5 in.) long x 150mm (6 in.) wide x 1.59mm (0.0625 in.) thick copper sheet that absorbs heat from the asphalt pavement. The lower end of the copper has a 63mm (2.5 in.), 90-degree bend, where it meets the TEGs. Copper was selected because it is an excellent heat conductor and has a high thermal conductivity. Copper is also very durable and has a specific heat of 385 J/kg C at 25°C (Chase, 1998). Multiple on-line sources cite a density of 8.96 g/cm^3 and a thermal conductivity of 401 W/m-K at 0°C. This copper sheet connects to two TEGs, which are electrically connected in parallel, by a thin layer of thermal paste (Fig. 3.1b).

The role of the copper plate is to deliver heat to the TEG so the upper surface of the TEG becomes much warmer than its bottom surface. To decrease losses along the copper, styrofoam insulation was added to the solar harvester. The R value of the insulation was approximately 2.8. The insulation was added to the 150mm (6 in.) bent part of the copper plate on both sides. The two insulation pieces were wrapped in electrical tape to mimic a seal around the insulation. An adhesive was used to hold the insulation in place. The insulation enables heat transfer to stay within the vicinity of the copper.

Heat Sink

Attached to the bottom side of the TEGs was an aluminum heat sink, which is used to dissipate the heat away from the TEGs (Fig. 3.1). Dissipating the heat away from the TEG allows for a greater temperature difference between the two sides of the TEG, producing an electrical current for sustainable power generation. The heat sink is attached to the colder (bottom) side of the TEG. The heat sink is 180.3mm (7.1in.) long x 99mm (3.9in.) wide x 45.7mm (1.8in.) tall.

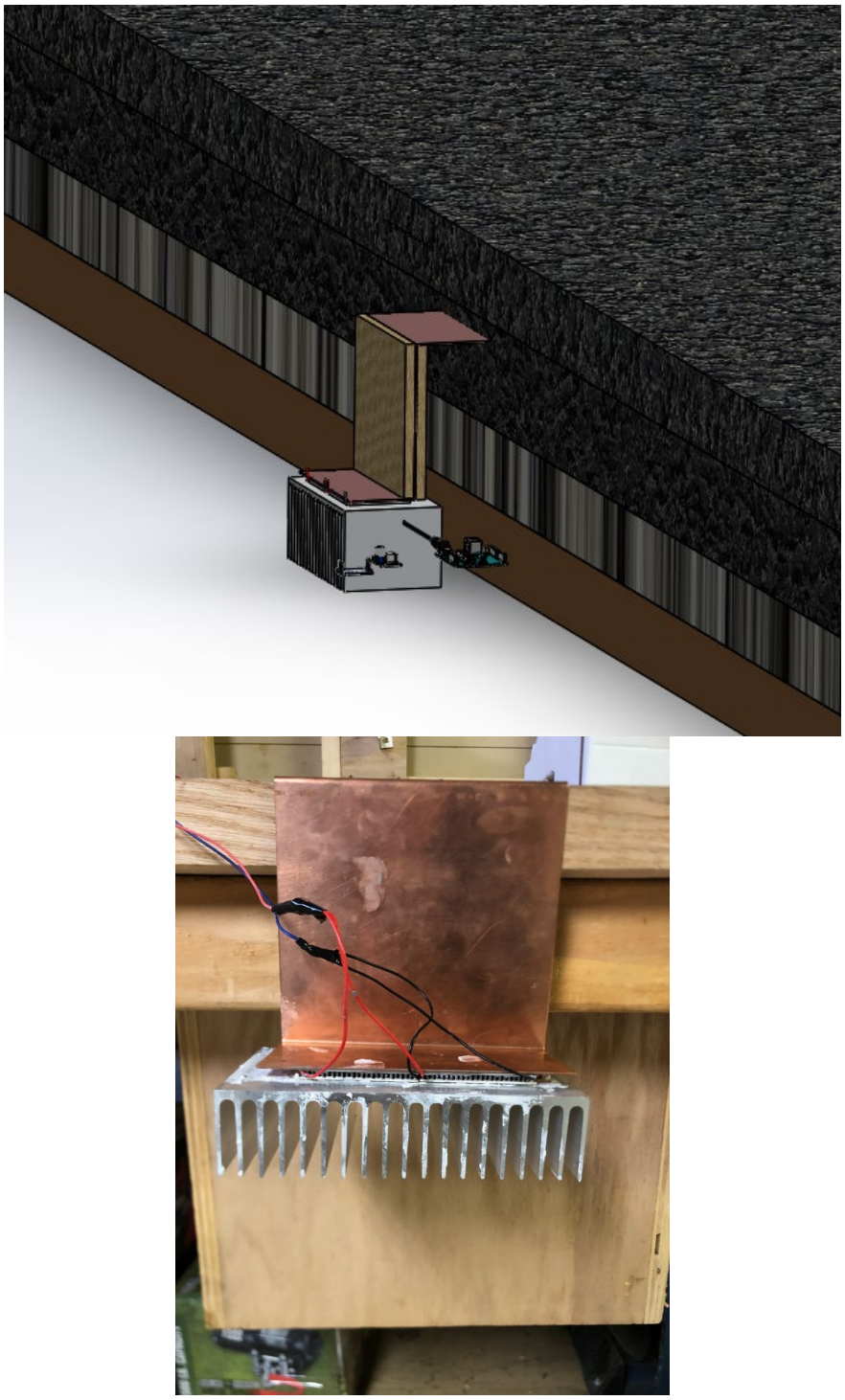

Figure 3.1. Solar energy harvesting system. (a) Cartoon of the harvesting system depicted next to an asphalt pavement. (b) Photograph of the TEGs between the copper plate and heat sink during benchtop testing. Pairs of black and red wires indicate the parallel physical and electrical geometries.

3.3 Apparatus to Use Solar Energy – Strain Sensing as an Example

Electrical energy must be used in real time unless a reservoir such as a rechargeable battery is present to utilize the electrical voltage and current. As a demonstration that energy harvesting can work, and as an added benefit in its own right, the energy harvesting apparatus was used to power a strain sensor that can monitor pavement durability.

The system to power and activate the sensor requires a steady voltage within a narrow range. Thus electrical circuitry and hardware was implemented to employ the TEGs as the power source. Programming of the strain sensor controller (the "Arduino" board) was also required.

Boost Converter

A boost converter is used to amplify the voltage of the solar apparatus and to keep the available voltage around 7 volts. It can take an input voltage of 2 to 24V and make an output of 5 to 28V. Without the boost converter, the TEGs would only be able to produce a certain temperature-dependent voltage that is not a constant power to supply the Arduino. The TEGs are then connected to a boost converter to amplify the voltage produced by the TEGs. A boost converter allows a low voltage to be converted to a higher voltage easily while stepping down the current. The TEGs must maintain an output voltage of at least 2 volts to power the boost converter. This boost converter is connected directly to an Arduino Uno board to allow programming of a road performance monitoring sensor.

Analog Digital Converter

An HX711 analog digital converter is used to power the Wheatstone bridge connection sensor, whose characteristics and specifications are listed in Table 3.1. The converter easily converts the analog signal of the strain sensor into a digital signal, to allow electrical signals for data processing purposes. Without the digital converter, the signal from the sensor would not be easily readable.

Table 3.1. Characteristics of Dynatest PAST sensor

Specifications				
Type	PAST II (For AC or PCC)		PCCST (for PCC only)	
Range	Up to 1500 μstrain		Do.	
Configuration	Single strain gage (1/4 brigde)		Do.	
Cell material	Epoxy—Fiberglass		Do.	
Coating	Epoxy—Silicone—PFT—Titanium		Epoxy—Silicone—PFT	
Resistance	120 Ω ±1.0 %; GF=2.0		Do.	
Voltage	Up to 12V (full bridge)		Do.	
Temperature	–30° to 150°C	–22° to 300°F	–10° to 60°C	14° to 140°F
∑E-modulus	≈ 2200 MPa	≈ 320 ksi	14,000 MPa	≈ 2000 ksi
Cross section	≈ 0.5 sq. cm	≈ 0.078 sq. in	0.25 sq. cm	≈ 0.04 sq. in
Cell Force	0.110 N/μstrain	≈ 0.024 lbf/μstrain	0.35 N/μstrain	≈ 0.08 lbf/μstrain
Fatigue life	Theoretically up to 10^8 cycles		Do.	
Service life	Typically > 36 months		Do.	

Note: Additional information is at the manufacturer web page, https://www.dynatest.com/pavement-strain-transducers-past

Arduino Uno Board

The Arduino Uno is the control behind the solar apparatus. It is a microcontroller-based board that can be easily programmed to control sensors via an Arduino code written in a form of Java. The Arduino requires an input voltage of 7 to 12 volts, so the boost converter is required to maintain the minimum voltage of 7 volts. The Arduino Uno is then connected to an HX711 Analog Digital Converter to power the roadway sensor.

Wheatstone Bridge Sensor – 5 kg Load Cell

The Wheatstone bridge circuit is attached to the Arduino board. This sensor chosen was a 5 kg load cell (Fig. 3.2). It contains a Wheatstone bridge connection, which is accurate in measuring very low resistances without requiring a lot of power (Table 3.1).

Figure 3.2. Dynatest Wheatstone bridge connection sensor

3.4 Procedure to Build Solar Harvester

The two TEGs were connected in parallel by connecting the positive and negative wires with solder. Thermal epoxy was applied to the bottom end of the copper plate to act as an adhesive for the TEGs. The 2-bond epoxy was mixed together with a stirring stick to ensure a proper homogenous mixture. The epoxy was then placed onto the hot side of the TEGs and attached onto the lip of the copper plate. After drying of the epoxy, shrink tubes were added to the negative and positive leads of the TEGs to secure the connection. The heat gun was applied to the shrink tubing which allowed the tubing to connect to the wiring. This shrink tubing replaced the black electrical tape and would ensure proper a moisture barrier from temperature changes. The epoxy was set for 24 hours to allow proper drying time (McCarthy et al. 2000; Purohit et al. 2013).

Next, the thermal heat sink was attached to the cold side of the TEG with the epoxy from earlier. Another 24 hours was required to allow the heat sink to dry completely. Styrofoam insulation with an R value of 2.8 was then cut out and attached to both sides of the 150mm (6 in.) tall section copper plate. Electrical tape bonded the copper between the two pieces of insulation. Another section of Styrofoam was also attached to the bottom side of the 470mm (18.5 in.) section. The insulation allows the heat loss from the sides and bottom the copper plate to be minimized, transferring the heat to the TEGs rather than to the surrounding pavement. An adhesive was used to hold the insulation in place.

The positive and negative ends of the TEGs were then soldered to the input side of the DC-DC boost converter. The boost converters set screw was turned to maintain a correct input voltage of 10 volts for the Arduino board. The Arduino board can be powered from 7-12 volts of power supply. The boost converters output pins are then soldered to a DC power cable (18 AWG), connecting into the DC barrel jack, allowing power to the Arduino Uno. The Arduino then connects to HX711 analog digital converter and the output connects to the 5kg load cell sensor (Karsilaya et al. 2018). Code for the load cell was written in Java using the Arduino software. This code can be changed and altered depending on the type of sensor used.

3.5 Cost Analysis

Some components were purchased to build solar harvester, and a strain sensor was purchased as summarized in Table 3.2.

Table 3.2. Costs of solar harvester and sensors

(a)Solar Harvester

Item	Cost
Thermo-electric generator model TXL-287-03	$236.80
Copper Plate (0.0625” thick x 6.5” W x 27” L)	$ 76.46
DC-DC Boost Converter	$ 2.00
Analog Digital Converter	$ 7
Heat Sink	$ 15
Thermal Paste	$ 7.99
Arduino Uno	$ 20

DC Power Cable	$ 9
TOTAL	$374.25

(b)Sensors

Item	**Cost**
5 KG Load Cell Sensor	$ 13
Dynatest PAST Sensor	$755
TOTAL	$768

3.6 Procedure to Install Solar Harvester and Sensor in the Field

To install the solar harvester and strain sensor, a cross section of asphalt pavement structure was developed as shown in Figure 3.3. There was a preliminary survey with URI Facility officers at the Plains Road Extension on May 8, 2020. When a contractor cut out pavement sections, solar harvester and strain sensor were installed on June 29, 2020.

Figure 3.4 shows connections among the TEGs, boost converter, Arduino Uno, amplifier, and load cell sensor. Together, these units constitute the electronics of the energy harvesting system. They were encased within an irrigation protection box for use in the field in order to protect them from moisture, rain, snow, and groundwater.

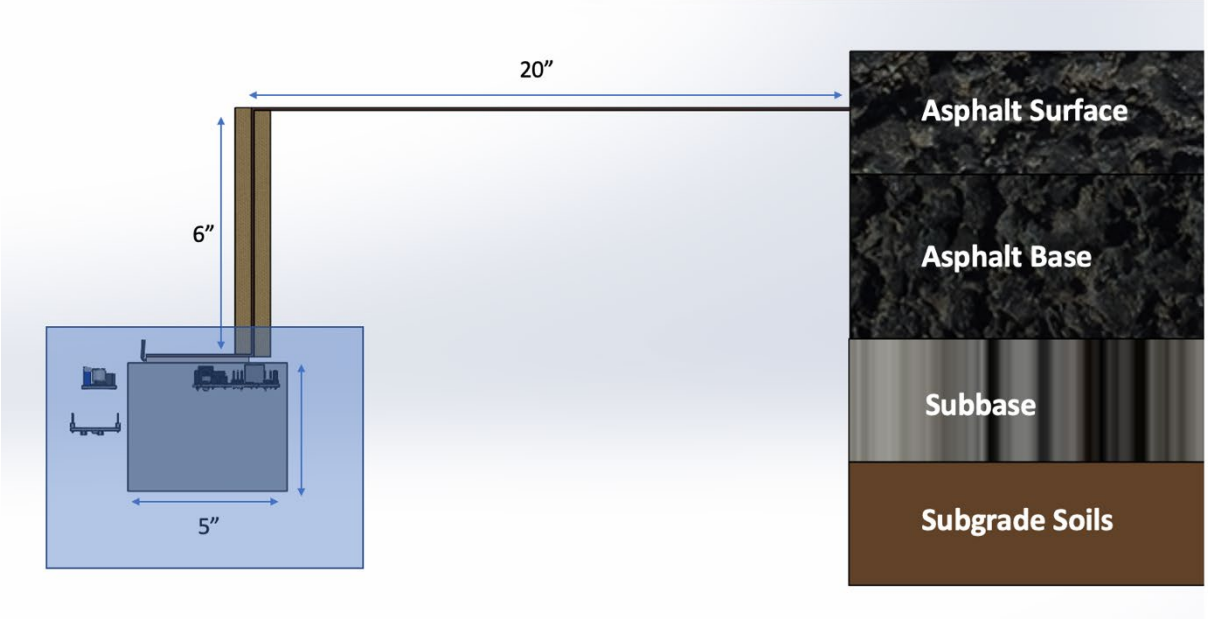

Figure 3.3: Cross section of Solar Harvester, embedded in shoulder of road 25 mm (1in) below asphalt surface

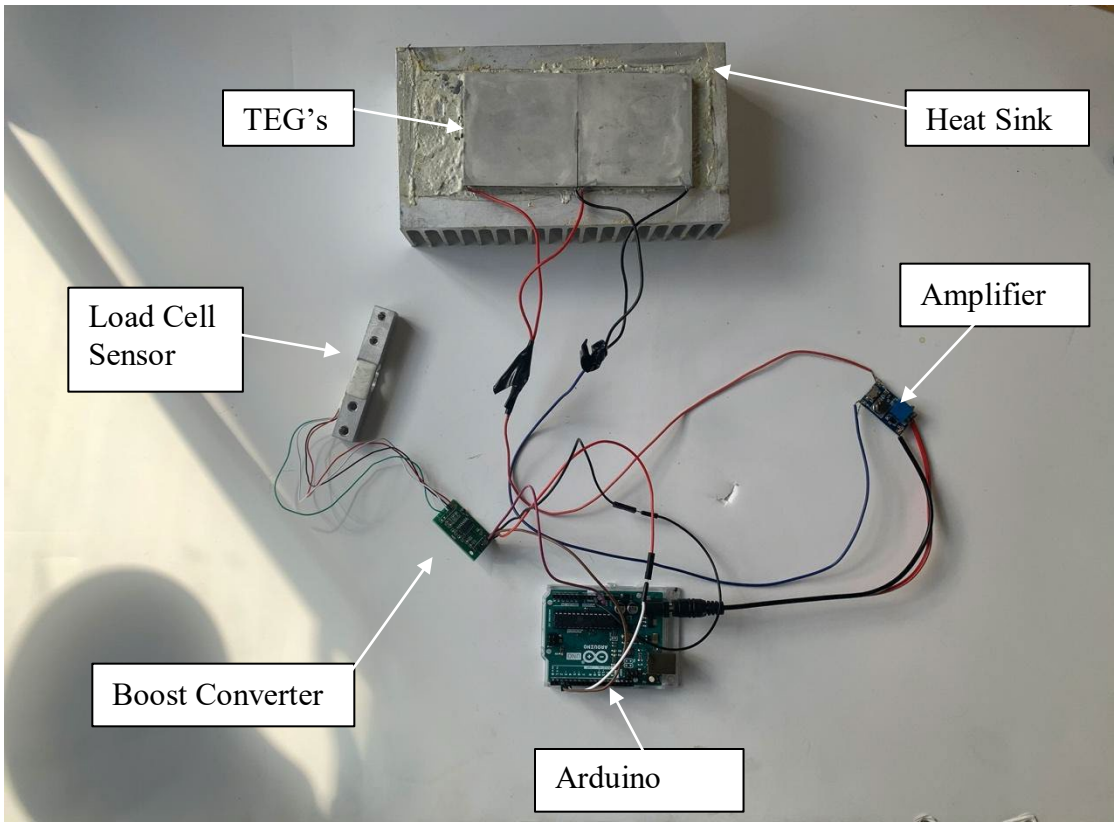

Figure 3.4: Connections between TEGs, Boost converter, Arduino Uno, Amplifier, and load cell sensor

3.7 Verification Before Field Installation

In a laboratory-scale test of the electronics for powering the sensor, two AA batteries were connected in series as an initial test for a power supply to the Arduino Uno. The batteries were soldered to the boost converter and then the DC cable jack produced a current of approximately 200 mA, which successfully powered the Arduino.

The solar energy harvester was tested in the laboratory by applying a heat gun to the top layer of the copper. The copper was heated to approximately 54ºC (130º F). The copper was able to effectively transfer heat to the top layer of the TEG, resulting in a power generation of 3 volts. This voltage exceeds the minimum two volts required for the boost converter, resulting in a powered Arduino. Varying the heating rate altered the temperature on the upper surface of the TEGs, which subsequently altered the voltage generated (Fig. 3.5). Even a hot-side temperature of 32.2ºC (90ºF) was enough to generate some voltage when the cold-side temperature was 23.3ºC (74ºF).

The load cell and Arduino were tested by using the five-volt USB jack on the Arduino and connecting it to a computer. This code allowed the Arduino to property read any loads (in grams) the sensor experiences; with collecting data continuously. Examples of these data are in Fig 3.5.

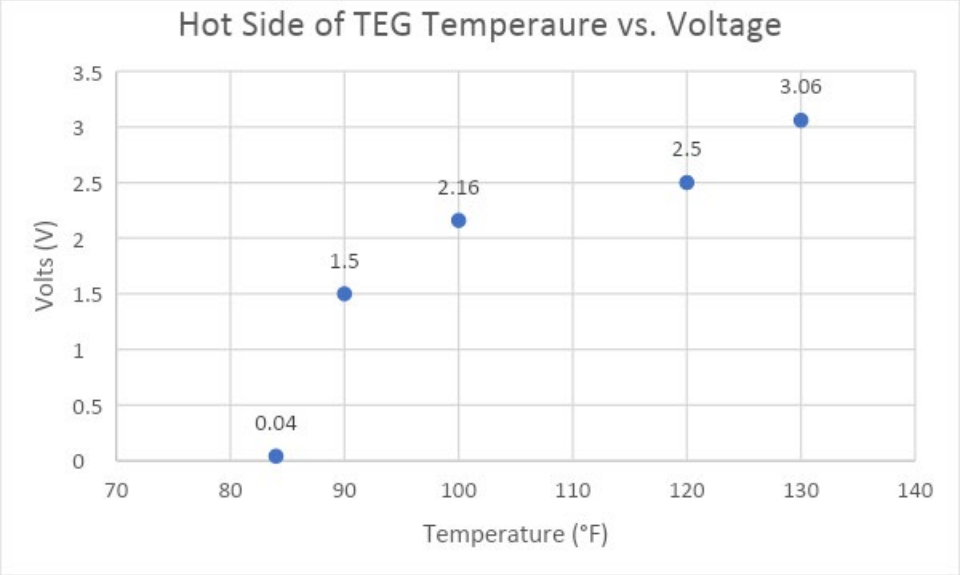

Figure 3.5: Temperature of the hot side of TEG with its corresponding voltage; ambient air temperature 23°C (74°F)

3.8 Installation

The solar harvester was installed along Plains Road near the URI campus on July 29, 2020. The site was chosen to satisfy requests from the URI facilities office, who kindly incorporated the construction work into the scope of work of an existing project elsewhere at the university. Plans for the installation are shown in Fig. 3.6. A realization of the plans on the road and shoulder, prior to construction, is shown in Fig. 3.7.

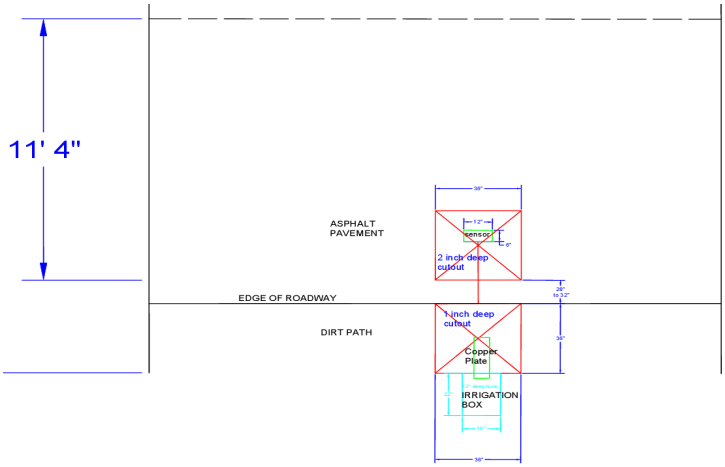

Figure 3.6. Plans for the location, layout, and geometry of the installed energy harvester and strain sensor on Plains Road in Kingston, RI.

Figure 3.7. Markings for the saw cuts for strain sensor (in the road) and energy harvester (in the shoulder) on Plains Road in Kingston, RI.

The first step was to dig a hole (Fig. 3.8) for the irrigation protection box to be inserted, which holds the electronics of the harvester. The hole was dug to the height of the irrigation box to make it flush with grade. The dirt was then back filled and compacted to hold the irrigation box securely. A 900 x 900 x 106 mm (36 x 36 x 4 ¼ in.) section of pavement was saw cut and removed from the road for the strain sensor. Next, the copper plate was inserted into the box with temperature gauges along the top, middle, and end section of the top surface. This allows for data collection of the varying temperatures along the copper heat plate.

Figure 3.8. Digging a hole for the irrigation box in the shoulder of Plains Road. From left Austin DeCotis, Stephan Zaets, Kevin Lapierre (digging), K. Wayne Lee (standing where the sensor will be installed).

The Dynatest strain sensor was placed into the base of the pavement cutout with the middle section of its H bar parallel with the roadway. The sensor was placed within the average passenger-side wheel path. The wiring of the sensor was placed in a 6¼ mm (¼ in.) sawcut line and sealed with silicon epoxy. Asphalt pavement was carefully placed over the sensor and hand tamped due to the sensitivity of the sensor. The remainder of the asphalt cutout was filled and compacted with a compacting machine, keeping away from the sensor. The asphalt temperature reading just before placement was recorded to be 110°C (230°F). A 50mm (2 in.) thickness of asphalt was then placed over the copper apparatus. It was compacted with the hand tamp and then properly dried.

The next day, a hole was cut into the irrigation box to allow the end of the sensor wiring to be accessible in the irrigation box. The irrigation box has two bolts and two caps to make the top cover air/watertight.

3.9 Strain Measurement

The installed energy harvester and strain sensor are now ready for in-field experiments. As a start, the sensor can be tested by using a P-3500 Strain indicator provided for the project by Kevin Broccolo of URI Civil Engineering. The wires connect into the wire jacks and the strain can be monitored.

3.10 Summary and Future Works

Further testing is needed to evaluate this implementation of the energy harvesting device into the roadway. Now that the solar harvester has been installed into the shoulder of a roadway, the ability of heat transfer to generate electrical energy needs to be tested in this real-world application. The temperature difference between the two TEGs will generate the required voltage to operate the roadway sensors. To enable output voltage by the TEGs below the asphalt surface layer, the harvester was installed with the copper plate 25mm (1 in.) below the top layer. This allows temperature difference readings as well as maximum power output voltage. This copper plate will be heated from the sun heating the asphalt surface layer and transferring the energy into the harvester system.

During installation of the solar harvester apparatus, multiple K type thermocouples were placed among the solar harvester in the following areas:

1. Top part of road surface
2. Top of copper plate along two ends and middle
3. Hot temperature side of TEG junction
4. Cold temperature side of TEG junction
5. Cold temperature sink portion
6. Intermediate points along copper that transfers heat to/from the semiconductor, but not near it
7. Any sort of measurement in duplicate or triplicate for reliability.

These thermocouples will allow data to be collected. Subsequent analysis will enable estimating where thermal losses occur. Optimizing the harvester for efficiency and sustainability are top priorities.

RITRC recommends that a SD card or Bluetooth receiver be implemented into the solar harvester unit. This will allow data for retrieval to be stored without an external power source (i.e., computer), allowing the harvester to operate freely. The SD card/USB will be able to store the information from the pavement strain transducer or other structural health monitoring sensors. Data retrieval would be achieved simply by unplugging the card from the harvester unit and uploading it to a computer.

RITRC also recommends that the Dynatest Pavement Strain Transducer gets installed into the asphalt surface layer for strain monitoring of the roadway. This sensor is capable of 100,000,000 cycles and has a service life that exceeds 36 months.

Another recommendation is a box for the Arduino itself so it can be mounted inside the irrigation box without any movement of the electronic components. A box can be easily printed using the 3D printers if an appropriate size is not found in a commercial source.

This solar apparatus will allow any type of roadway sensor/road monitoring device to be installed. Any sensor can be programmed and configured into the Arduino board.

The solar apparatus can be further developed by creating a "manhole" for the electrical configuration of the harvester. A manhole will enable access to the electrical connection to allow different sensors to be tested from the Arduino board. It also prevents outside parameters from damaging the electrical connections. The recommended box configuration should be like an irrigation system box because it forms a watertight seal. Water cannot be allowed to enter the box because the electrical components would be compromised from the environment. The box will have to be approximately 300mm by 300mm (one foot wide by one foot) deep to allow proper room for the configuration. A small hole will have to be drilled through the box for the sensor wires going into the roadway. This hole can then be watertight by corking the remaining gaps in the hole.

It is also recommended adding an energy storage device such as a capacitor to the TEG's output wires to store voltage that is produced. The TEGs send current to the boost converter, but if there is not a continuous supply of two volts, the boost converter will not amplify the voltage to power on the Arduino Uno.

The Arduino can be turned on by a powered button that gets pressed/reset. Once the copper plate receives the required voltage from the heat generation, the Arduino can be turned on. To communicate with the Arduino board in the current set-up, a USB cord gets plugged into the Arduino with the other end into the computer. The software program *Arduino* should then be opened on the computer to read data from the apparatus. Code must be written in the software to run the sensor properly.

Chapter 4: Thermodynamic Analysis of Solar Energy Harvesting Processes

The goals of thermodynamic modeling work are to assess the viability of the different energy harvesting strategies that were considered. More calculations were done for the thermal strategy of extracting heat directly than for the thermoelectric energy generation approach.

4.1 Finite Element Modeling of Heat Flow from Asphalt into a Cooling Water Pipe

Modeling was conducted by using COMSOL software to estimate the impact on asphalt temperature of cool water flowing through a pipe immersed in the asphalt. Default choices within the software were chosen for asphalt physical properties. An example of the results is shown in Figure 4.1. It depicts a cross section of the cool pipe. Water flow was not incorporated directly; instead the pipe surface was set to a cool temperature. Heat was pulled into the pipe from its immediate surroundings, as indicated by the strong color change around it for a distance of approximately one pipe diameter. A smaller temperature drop occurred over distances of a few pipe diameters. At long distances, no impacts on the asphalt temperature were found in the calculations.

This shows that a macroscale calculation is consistent with the observations in the experiments. A temperature change that is induced into the pavement by external heating can be altered by providing a cooling medium that flows through a pipe buried into the asphalt. Physical proximity to the pipe is important in terms of extracting energy from the asphalt and thereby warming the water.

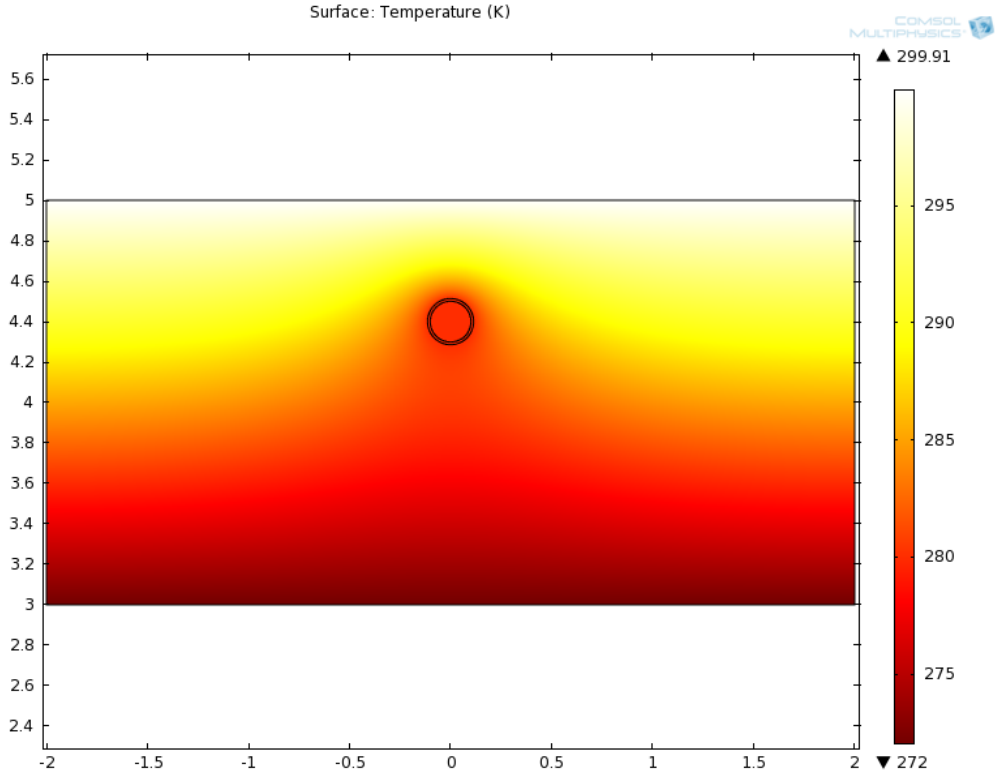

Figure 4.1. Calculated temperature profile for asphalt around a cooling pipe.

4.2 Theoretical Efficiency of Extracting Heat from Asphalt as Work

A desired intent of the thermal strategy was to convert available heat, which could be extracted into water, into useful work through a "heat engine" in the form of a conventional power cycle. Large scale examples include combusting fossil fuels to create heat, using that heat to form high-pressure steam, extracting energy in a turbine in the form of useful work, and rejecting the remaining heat at a lower temperature and pressure.

The best-case scenario for such a power cycle can be calculated by considering a Carnot cycle, in which all real-world losses are ignored, heat transfer is considered to be perfect (no driving force required, no temperature change during heat transfer, infinite time and area available, no entropy generation). With these assumptions, the *thermal efficiency*, or (work available) per (heat added), is written as

$$\eta_{th} = 1 - T_{low} / T_{high} \tag{4.1}$$

which relies only on the temperature (in Kelvin) of the heat source and heat sink. Employing conditions of 60°C (pavement surface) and 15°C (ground) leads to

$$\eta_{th} = 1 - (15 + 273.15)/(60 + 273.15) = 13.5\% \tag{4.2}$$

This maximum possible efficiency of 13.5% compares to maximum efficiencies of more than 60% in a commercial power plant. 86.5% of all available heat is discarded even before accounting for any real-world inefficiencies in the process. The heat engine approach also assumes that some sort of cool reservoir is available to accept the heat. **Without such a way to remove heat from the circulating water, it is not possible to attain this small efficiency even in the absence of other losses or real-world factors**. The Carnot efficiency is certainly discouraging in terms of considering any possible extraction of energy via a heat engine.

4.3 Modeling of Energy Added to Cooling Water by a Pump

The heat extraction experiments suggested that heating effects inducted by pumping water through immersed pipes were potentially a concern. In particular, it was found that the water warmed to a higher temperature than that of the artificially heated pavement. This indicates an energy source other than heat extracted in order to cool the surrounding pavement. Thus the pump energy was computed two ways. One used approximate pump conditions to estimate the energy input rate and consequential temperature change. Another used the heating rate in different experiments to infer a heat input rate from the pump. Results from both calculations were self-consistent.

The experiments circulated water from a large container through the pipe that was surrounded by asphalt pavement. Water flowing out was added back to the container. Either 3L or 5L of water started in the container. The temperature of the water in the container was measured; no other water temperature or flow rate data are available. A pump caused this flow to occur.

The work that is done by the pump to cause the flow can be approximated as

$$\dot{W}_s = \Delta(P\dot{V}) \approx (P_2 - P_1)\dot{V} \tag{4.3}$$

A pressure rise of 1 bar applied to a water flow rate of (1 L/min) provides (1 bar)(1000 cm^3/min) = 100 J/min of work. If the pump is 60% efficient at converting input energy into useful work, then the actual input energy equals Ws/0.60 = 2.8 J/s of energy input. Applying this energy input rate to 5 L of water can raise its temperature by approximately

$$\left(\frac{2.8\ \text{J}}{\text{s}}\right)\left(\frac{3600\ \text{s}}{\text{hr}}\right)\left(\frac{\text{cal}}{4.184\ \text{J}}\right)\left(\frac{\text{g-C}}{1\ \text{cal}}\right)\left(\frac{\text{cm}^3}{1\ \text{g}}\right)\left(\frac{1}{5000\ \text{cm}^3}\right) = 0.48\ ^\circ\text{C/hr} \tag{4.4}$$

Over 12 hours, this is a rise of 5.8°C or 10.4°F. Considering all of the energy input as contributing to temperature rise is reasonable because the kinetic energy of flow and the pressure rise are ultimately lost after the water circulates through the pipes immersed in the asphalt and returns to the storage container.

A similar analysis can infer the energy input rate of the pump from experimental measurements of temperature rise for 3 L and 5 L of water over 12 hours, when the asphalt is not heated. When the circulating water is considered as a thermodynamic system, the First Law indicates that shaft work raises the internal energy of the water,

$$\dot{W}_s = M\frac{d}{dt}\hat{U} \approx \frac{\Delta\hat{U}}{\Delta t} \tag{4.5}$$

The change in internal energy U (or energy per mole, with the carat) can be determined by using the heat capacity. Here we set the reference point for internal energy such that internal energy equals zero at the initial temperature of the water. We also assume that the heat capacity at constant volume and at constant pressure are the same for the water, which is reasonable for a liquid, and we use a temperature-dependent heat capacity from Dahm and Visco (2015). This leads to

$$\Delta\hat{U} = \int_{T_0}^{T} R\left(C_p / R\right)dT = R\left(AT + \frac{B}{2}T^2 + \frac{C}{3}T^3 + \frac{D}{4}T^4\right)\Bigg|_{T_0}^{T} \tag{4.6}$$

R = 8.314 J/mol-K indicates the universal gas constant, and parameters A, B, C, D are listed in Table 4.1. Temperature T is in Kelvin. With this approach, measured data for the temperature rise from T_0 to T can thus provide the rate of shaft work that is applied in the pump.

Table 4.1 Heat capacity parameters for water (Dahm and Visco, 2015)

A	B	C	D
6.1152	2.5627×10^{-2}	-7.59393×10^{-5}	7.80258×10^{-8}

Two experiments were conducted to test the pump energy input. In an experiment with 3 L of water, the reservoir temperature rose from 65°F to 105°F. In an experiment with 5 L of water, the reservoir temperature rose from "about 65°F" to 93°F. Both experiments used the same pump and the same pipes through room-temperature asphalt. Calculation results for these cases are listed in Table 4.2. According to these data, the pump added energy at a rate between 6.5 and 7.5 W. Because the precise initial temperature had not been noted for the experiment with 5 L of water, another calculation considered a different initial temperature. Using 69°F rather than 65°F as the starting point for 5 L leads to a consistent rate of 6.5 W for the energy input rate from the pump.

Table 4.2 Calculation results for pump energy input

Volume H_2O	T_{in}	T_{out}	ΔU	Total ΔU	Pump work
3 L	65°F	105°F	1677.3 J/mol	279.03 kJ	6.46 W
5 L	65°F	93°F	1173.6 J/mol	325.40 kJ	7.53 W
5 L	*69*°F[a]	93°F	1006.1 J/mol	278.95 kJ	6.46 W

(a) This initial water temperature is an estimate that shows equivalent pump work.

These calculations reiterate a drawback of this approach that was witnessed in the experiments. Over time, the water that is circulated in order to cool the asphalt can be heated simply because of the mechanical motion and the pumping action that is required to make the flow occur. While the water can remove heat initially from asphalt that is heated during daily heating cycles, the ongoing energy input to continue the water circulation can raise the water temperature to a point that it is *adding* energy into the asphalt, rather than removing it.

4.4 Example of Heat Flow Condition during Thermoelectric Energy Harvesting

The energy harvesting system that uses a thermoelectric generator (TEG) was described in Chapter 3. It relies on bringing heat from a hot pavement surface down to the top surface of a TEG. Simultaneously the opposite side of the TEG is in thermal contact with cooler temperatures below the road. The temperature difference causes a voltage across a semiconductor. Connecting the opposite ends through a circuit allows for electrical work to be performed.

The heat is brought to the TEG through a copper plate. A wide upper surface warms the copper with an intent of it reaching the pavement temperature. Insulation along its sides is intended to allow heat to transfer *through* the copper and thus down from the surface while simultaneously blocking heat flow from the copper *into* the surrounding asphalt that is less hot.

A first calculation illustrates the rate that thermal energy can be carried through the copper to the TEG. Applying the First Law of thermodynamics within a thin section of the copper (the "system") indicates that heat flow changes the internal energy of the copper,

$$dQ = Md\hat{U} \approx MC_p dT \tag{4.7}$$

This is analogous to equation (4.5) for the water pump because both work and heat can provide energy that flows into or out of a system. The driving force for heat flow through an insulated portion of the copper is that there is a temperature difference between the asphalt near the surface and the buried location of the TEG. Fourier's Law of heat conduction expresses this driving force by using the thermal conductivity of copper,

$$\frac{\dot{Q}}{A} = k\nabla T = k\frac{dT}{dx} \tag{4.8}$$

Multiple sources cite a thermal conductivity k = 401 W/mK near room temperature for copper. Its heat capacity is Cp = 0.385 J/g°C at 25°C (Chase, 1998).

An estimate of the heat transfer rate can be made by replacing the derivative in equation (4.8) with finite differences in temperature and position. Here we assume a linear temperature gradient between 140°F

(60°C) and 68°F (20°C) for simplicity along the 6" length of copper. Inputting the dimensions of the copper plate and employing unit conversions as needed indicates

$$\dot{Q} = kA\frac{dT}{dx} = (6.5 \times 0.0625\ \text{in}^2)(401\ \text{W/mK})\left(\frac{40\ \text{K}}{6\ \text{in}}\right)\left(\frac{0.0254\ \text{m}}{\text{in}}\right) = 27.6\ \text{W} \qquad (4.9)$$

We note that the temperature change of (60 – 20°C) = 40°C is identical in degrees Kelvin. The first factor on the right side provides the cross sectional area of copper normal to the flow direction.

This calculation indicates that heat flow can proceed as quickly as 27.6 W between hot pavement and a cool TEG. The experiments of chapter 3 involve work production rates that are closer to a range of 1 – 3 W. It can be concluded that sufficient energy is potentially available through heat transfer through the copper.

4.5 Example of Heat Flow Dynamics during Energy Harvesting

A more detailed example of the heat flow dynamics within the vertical section of the copper plate during energy harvesting can be obtained by combining equations (4.7) and (4.8) into Fourier's second law of heat conduction,

$$\frac{\partial T}{\partial t} = \frac{k}{\rho C_p}\nabla^2 T \qquad (4.10)$$

which can then be solved for the time- and position-dependence of temperature in the copper between positions x=0 at the upper part with a more hot temperature (such as 140°F or 60°C) and $x=L$ at the lower part with a more cool temperature, such as 68°F or 20°C. Solving this differential equation requires two boundary conditions in position and one initial condition in time. A possible initial condition specifies this lower temperature throughout the copper at $t=0$. At $x=0$, assume the hot temperature is maintained. To track the rate that the copper can heat up, neglect heat transfer out of the copper at $x=L$. From equation (4.8), this sets the temperature position derivative to zero.

When the thermal conductivity, mass density, and heat capacity are sufficiently independent of temperature, equation (4.10) can be solved analytically by using the separation of variables method. Briefly, it first is rewritten in terms of a dimensionless change in temperature compared to the warm and cool extremes,

$$\theta = \frac{T(x,t) - T_0}{T_1 - T_0} \qquad (4.11)$$

Equation (4.10) remains the same with this substitution, other than T being replaced by □. The boundary conditions become □ = 0 at $x=0$ at all times, □' = 0 at $x=L$ at all times; the initial condition is □ = 1 everywhere at $t = 0$.

Next, the function □(x,t) is written as a product of a time-dependent function $f(t)$ and a position-dependent function $g(x)$. Substituting these into equation (4.10), applying the derivatives, and rearranging leads to the differential equations

$$\frac{\rho C_p}{k}\frac{1}{f}\frac{\partial f}{\partial t} = \frac{1}{g}\frac{d^2 g}{dx^2} = -(\text{constant}) \qquad (4.12)$$

The two equations for f and g must equal a constant because they are equal for various times and positions, with time affecting only the f equation and position affecting only the g equation. The negative sign in front of the constant is chosen for convenience later. Solving each side, applying the initial condition, and applying the boundary conditions leads to the following equation for the temperature change,

$$\theta = \frac{T(x,t)-T_0}{T_1-T_0} = \sum_n \frac{2}{\pi}\frac{1}{(n-1/2)} \exp\left(-\frac{k}{\rho C_p}\frac{\pi^2}{L^2}(n-1/2)^2 t\right) \sin\left(\pi(n-1/2)\frac{x}{L}\right) \quad (4.13)$$

Theoretically, the integer n spans from 1 to infinity. In practice, the exponential term ensures that contributions become negligible for large enough n at long enough times. Here, a maximum of 200 terms was chosen. The ratio ($k/\square C_p$) is called thermal diffusivity. It is often notated as $\square$ and has units of (length squared per time).

As an example of using equation (4.13), the temperature profile along the length L = 6 in of the copper plate going into the ground can be calculated. Temperatures of T_0 = 140°F = 60°C and T_1 = 68°F = 20°C are specified. Thermal conductivity k and heat capacity C_p are listed near equation (4.8) above and in chapter 3. The density $\square$ = 8.96 g/cm^3.

Figure 4.2 shows results from the model over times from 0 to 300 seconds. As a consequence of the high thermal diffusivity of copper, which is largely attributed to its high thermal conductivity, the temperature rises rapidly along the copper plate. The temperature is predicted to exceed 110°F over the first inch after only 10 seconds. The entire plate is predicted to reach 100°F after about 1 minute and 120°F after just over 2 minutes. After 5 minutes, nearly the entire plate has reached its upper surface temperature of 140°F. This suggests that the copper plate setup will be effectively at bringing heat from near the hot asphalt surface down to the TEG.

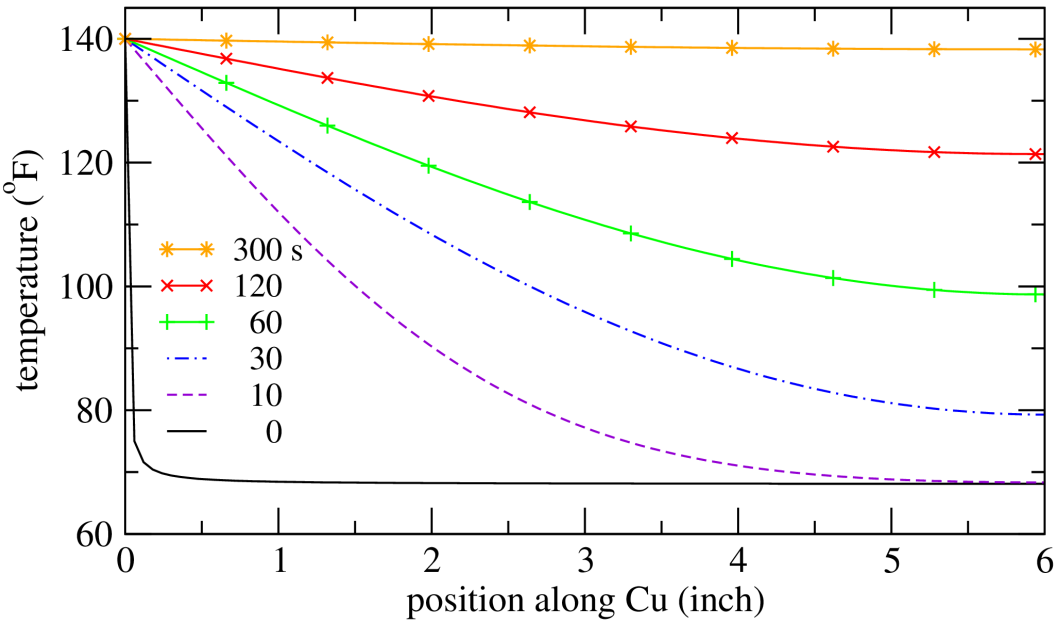

Figure 4.2. Model results for temperature within the vertical copper plate, assuming perfect insulation along the sides and an instantaneous rise to 140°F at the top.

While this model calculation is encouraging, it is not expected to correspond precisely with experimental measurements. It assumes that the temperature near the asphalt surface instantaneously reaches 140°F (60°C) at time zero, as does the horizontal copper plate. In reality, the asphalt will heat up over time due to incoming solar radiation, and some time will be required to transfer that heat into the adjoining copper. This would provide a less sudden driving force for bringing heat to the TEG.

The calculation also neglects heat losses into the neighboring asphalt through the insulation. Such heat losses would cause a temperature gradient across the copper plate in its thin dimension at each time. The better the insulation, the smaller this effect. The rate of heat conduction into the insulation from the copper and into the asphalt from the insulation would each mediate these effects. Indeed, the intent of the Styrofoam insulation is to minimize the extent of this heat flow.

Calculations were not performed for the extraction of heat from the TEG via the heat sink. Fewer details about the geometry and the physical relationship between the heat sink and the road subbase were available for the calculations.

4.6 Conclusions from Modeling

Several conclusions may be drawn from the modeling calculations. While it is true that circulating cool water through the asphalt via a pipe can potentially remove heat, the energetic costs of pumping that water can lead to a "reverse" situation in which the warming water is adding heat to the asphalt, rather than removing it. This experimental finding is not a fluke or an experimental error; it is consistent with the thermodynamics of fluid flow. The maximum possible efficiency of extracting energy, i.e. the Carnot efficiency, indicates that relatively little productive work can be done even if all other aspects of the system had no real-world engineering losses. Such a scenario is not possible, particularly within the constrained environment that is imposed by the costs and geometric scales of road construction and the relatively low economic value of the energy that could be obtained. A low-temperature heat sink for cooling the water would also be required.

A heat flow analysis of the TEG setup indicates that enough thermal energy flow is possible through the vertical copper plate to allow the TEG to generate electrical work at the desired voltages, though at low currents. A dynamic analysis shows that if the insulation works sufficiently well such that heat flow is channeled along the copper plate rather than through its sides, the temperature at the upper surface of the TEG can become very close to the upper pavement temperature. Thus it is reasonable to consider a hot-side temperature driving force that is near the hot temperature of an asphalt pavement surface that receives solar heating.

Chapter 5: Conclusions and Recommendations

After thorough examination of past experiments on heating water, the large pump being utilized was rapidly causing the water to heat up so much that the temperature of the water quickly became hotter than the surrounding where the pipe was placed in the pavement structure. During control testing (the testing without water being pumped through the pavement structure), the pavement layer at 100mm (4 in.) was only reaching peak temperatures of approximately 80ºF. However, during the control testing for the water, the pump was heating up the water to temperatures of 94ºF. With the temperature of the water already reaching much higher temperatures than the surrounding pavement, there is no possible way to cool down the pavement and to increase the temperature of the water. Optimum results were not achieved, but there is still a possibility this method could work with future refinement. First and foremost, a smaller pump that puts out less heat would need to be used to determine if the heat of the pavement structure can increase the temperature of water. Though it may be possible that a much smaller pump could sufficiently pump water through this small-scale lab experiment, even a small energy consumption rate (less than an LED light bulb) would warm the circulating water such that it could heat up the asphalt, rather than remove heat. Another consideration that could make this experiment more efficient would be using high intensity bulb and/or moving the height of the pipe in the pavement structure closer to the surface. This would increase the temperature of the pavement surrounding the pipe, which makes it more likely to increase the temperature of the water. However, in doing this it creates the potential for the embedded pipes to be damaged by traffic in a real-world situation. Moving the pipes any closer to the surface would likely require load testing to determine the structural adequacy of the setup. This system requires continuous validation utilizing the embedded conductive piping.

Another approach was continued to create an efficient asphalt pavement solar collector using thermoelectric generators. Thorough testing was needed to evaluate the implementation of the energy harvesting device into the roadway. The temperature difference between the two TEGs will generate the required voltage to operate the roadway sensors. Now that the solar harvester has been installed into the shoulder of a roadway, the ability of heat transfer to generate electrical energy needs to be tested in this real-world application. To enable output voltage by the TEGs below the asphalt surface layer, the harvester was installed with the copper plate 25mm (1 in.) below the top layer. This allows temperature difference readings as well as maximum power output voltage. This copper plate will be heated from the sun heating the asphalt surface layer and transfer the energy into the harvester system. Calculations show that this heat transfer is reasonable if heat flow along the plate into deeper asphalt layers can be neglected.

During installation of the solar harvester apparatus, multiple K-type thermocouples were placed among the solar harvester in the following areas: Top part of road surface, Top of copper plate along two ends and middle, Hot temperature side of TEG junction, Cold temperature side of TEG junction, Cold temperature sink portion, Intermediate points along copper that transfers heat to/from the semiconductor, but not near it, and any sort of measurement in duplicate or triplicate for reliability. These thermocouples will allow time and temperature data to be collected. Subsequent analysis will enable estimating where thermal losses occur. Optimizing the harvester for efficiency and sustainability are top priorities. An SD card or Bluetooth receiver was implemented into the solar harvester unit. This will allow data for retrieval to be stored without an external power source (i.e., computer), allowing the harvester to operate freely. The SD card/USB will be able to store the information from the pavement strain transducer or other

structural health monitoring sensors. Data retrieval would be achieved simply by unplugging the card from the harvester unit and uploading it to a computer.

Another recommendation is a box for the Arduino itself so it can be mounted inside the irrigation box without any movement of the electronic components. A box can be easily printed using the 3D printers if an appropriate size is not found in a commercial source. This solar apparatus will allow any type of roadway sensor/road monitoring device to be installed. Any sensor can be programmed and configured into the Arduino board.

The solar apparatus can be further developed by creating a "manhole" for the electrical configuration of the harvester. A manhole will enable access to the electrical connection to allow different sensors to be tested from the Arduino board. It also prevents outside parameters from damaging the electrical connections. The recommended box configuration should be like an irrigation system box because it forms a watertight seal. Water cannot be allowed to enter the box because the electrical components would be compromised from the environment. The box will have to be approximately 300mm by 300mm (one foot wide by one foot) deep to allow proper room for the configuration. A small hole will have to be drilled through the box for the sensor wires going into the roadway. This hole can then be watertight by corking the remaining gaps in the hole. It is also recommended adding an energy storage device such as a capacitor to the TEG's output wires to store voltage that is produced. The TEGs send current to the boost converter, but if there is not a continuous supply of two volts, the boost converter will not amplify the voltage to power on the Arduino Uno. The Arduino can be turned on by a powered button that gets pressed/reset. Once the copper plate receives the required voltage from the heat generation, the Arduino can be turned on. To communicate with the Arduino board in the current set-up, a USB cord gets plugged into the Arduino with the other end into the computer. The software program *Arduino* should then be opened on the computer to read data from the apparatus. Code must be written in the software to run the sensor properly.

The Dynatest Pavement Strain Transducer was installed into the asphalt surface layer for strain monitoring of the roadway. This sensor is capable of 100,000,000 cycles and has a service life that exceeds 36 months.

Thermodynamic modeling work confirmed that heating of the water by a pump should be expected. A combination of dynamic heat transfer and thermodynamics modeling indicates that the use of a copper plate should enable heat from near a pavement surface to reach a TEG that is further below the surface to enable a voltage-generating temperature difference to be obtained.

If the advanced technology approaches begun in this research are successful, they will enable pavement lifetime through extracting energy from an asphalt mix, enabling the asphalt to persist at a lower temperature. Sensing equipment that is powered through thermally generated electrical energy will enable for ongoing monitoring of road quality and stress-strain conditions without ongoing external power requirements. This *in situ* power generation enables technologies that are being pursued within other projects of the RITRC.

References

1. Akbari, Hashem. (2005). Energy Saving Potentials and Air Quality Benefits of Urban Heat Island Mitigation (PDF) (19 pp, 251K). Heat Island group Report, Lawrence Berkeley National Laboratory.
2. Chase, M.W. Jr. (1998). NIST-JANAF Thermochemical Tables, Fourth Edition, *J. Phys. Chem. Ref. Data*, Monograph 9, 1–1951.
3. Dahm, K.D. and Visco, D.P. Jr. (2015). *Fundamentals of Chemical Engineering Thermodynamics*. Stamford, CT: Cengage Learning.
4. Feng, J. and Ellis, T.W. (2003). 'Feasibility study of conjugated polymer nanocomposites for thermoelectric", Synthetic Metals, 135-136, pp 55-56
5. Han, R., Jin, X., and Glover, C. J. (2011). "Modeling Pavement Temperature for Use in Binder Oxidation Models and Pavement Performance Prediction". J. Mater. Civ. Eng., 23:351-359.
6. Karsilaya, A., Dessouky, S., and Papagiannakis, A. (2018). "Development of a Self-Powered Structural Health Monitoring System for Transportation Infrastructure" Publications. 27.
7. Lee, K.W. and Correia, A. (2010). "A Pilot Study for Investigation of Novel methods to Harvest Solar Energy from Asphalt Pavements," Final Report to Korea Institute of Civil Engineering and Building Technology (KICT).
8. Lee, K.W., Craver, V., Kohm, S. and Chango, H. (2010). "Cool Pavements as a Sustainable Approach to Green Streets and Highways, Proc. of the 1st ASCE T&DI Green Streets and Highways Conference, Denver, CO.
9. Lee, K. W. and Correia, A. (2011). "Investigation of Novel Methods to Harvest Solar Energy from Asphalt Pavements," Proc. of the 7th International Conference on Road and Airfield Pavement Technology (ICPT), Bangkok, Thailand, pp 1001-1008.
10. Lee. K. W., Correia A. and Park, K. (2012a). "Solar Energy Harvesting from Asphalt Pavement to Reduce Dependence on Finite Fossil Fuel Supplies" Final Research Report to Expressway & Transportation Research Institute (ETRI), Korea Expressway Corporation (KEC), ETRI-2011-3.
11. Lee, K. W., Yang, S. and Correia, A. (2012b). "Investigation of Novel Methods to Harvest Solar Energy from Asphalt Pavements," Proc. The ISAP International Symposium on Heavy Duty Asphalt Pavements and Bridge Deck Pavements, Nanjing, China.
12. Lee, K.W. and Kohm, S. (2014). "Cool Pavements," Chap. 16, Springer's Book on Climate Change, Energy, Sustainability and Pavements, Springer-Verlag, Inc., ISBN: 978-3-662-44719-2 _16. Editors: Gopalakrishnan, Kasthurirangan, Steyn, Wynand JvdM, Harvey, John (Eds.)
13. McCarthy, P., Li, W., and Yang, S.C. (2000). "New water-borne electroactive polymers for coating applications." Polymeric Materials Science and Engineering, 83:315-316.
14. Pinter E., Fekete, Z.A., Berkesi, O., Makra, P., Patzko, A. and Visy, C., (2007). "Characterization of Poly 3-octylthiophene/Silver Nanocomposites Prepared by Solution Doping," Journal of Physical Chemistry C 2007, 111, 32, 11872-11878.
15. Purohit, K., Yang, S. and Lee, K.W. (2013). "Polymer Thermoelectric Material for Energy Harvesting," Proc. US-Korea Conference (UKC), East Rutherford, NJ.

16. Racicot, R., Brown, R., and Yang, S.C. (1997). "Corrosion protection of aluminum allows by double-strand polyaniline" Syn. Met. 85, 1263.

17. Yang, S.C., Brown, R., and Sinko, J. (2005). "Anticorrosive coatings based on novel conductive polymers", European Coating Journal, 11, 48.

Transportation Infrastructure Durability Center
AT THE UNIVERSITY OF MAINE

35 Flagstaff Road
Orono, Maine 04469
tidc@maine.edu
207.581.4376

www.tidc-utc.org